SUPPORTING INFORMATION FOR

Alkali Cation Effects on Redox-Active Formazanate Ligands in Iron Chemistry

Daniel L. J. Broere,[*,†] *Brandon Q. Mercado,*[†] *Eckhard Bill,*[§] *Kyle M. Lancaster,*[‡] *Stephen Sproules,*[⊥] *and Patrick L. Holland*[*,†]

[†]Department of Chemistry, Yale University, New Haven, Connecticut 06520, United States

[‡]Department of Chemistry and Chemical Biology, Baker Laboratory, Cornell University, Ithaca, New York 14853, United States

[§]Max Planck Institute for Chemical Energy Conversion, Stiftstrasse 34-36, D-45470 Mülheim an der Ruhr, Germany

[⊥]WestCHEM, School of Chemistry, University of Glasgow, Glasgow G12 8QQ, United Kingdom

Corresponding authors:

patrick.holland@yale.edu

daniel.broere@yale.edu

Department of Chemistry, Yale University, 225 Prospect Street, New Haven, Connecticut 06520, United States

Table of contents

Experimental

General considerations. All reactions were performed under an N_2 atmosphere in an M. Braun glovebox maintained at or below 1 ppm of O_2 and H_2O. Glassware was dried at 160 ˚C under vacuum. Solvents were dried by passage through Q5 columns from Glass Contour Co., with the exception of THF, which was distilled under Ar from a potassium benzophenone ketyl solution. THF-d_8 was dried in a potassium benzophenone ketyl solution and distilled before use. Complex **1** was prepared as reported previously.[1] Na sand was obtained by exhaustive washing of a Na (25-35 wt %) dispersion in paraffin (Sigma Aldrich) with pentane. KC_8 was prepared by heating stoichiometric amounts of potassium and graphite at 140 °C under an argon atmosphere. Rubidium on graphite (RbC_8) was prepared by heating stoichiometric amounts of rubidium and graphite at 130 °C under an argon atmosphere. Cesium on graphite (CsC_8) was prepared by mixing stoichiometric amounts of cesium and graphite at ambient temperature under argon atmosphere.[2] *Caution: Reaction of cesium with graphite is highly exothermic becoming red-hot upon mixing and therefore should be in contact only with metal or glass supports. Warning: Alkali metals and their graphite intercalates KC_8, RbC_8, and CsC_8 are powerful reductants, which ignite on contact with air and moisture. Therefore, extreme care must be taken when synthesizing and handling these alkali graphite reductants!* ^{1}H NMR data were recorded on a Bruker Avance 400 or 500 spectrometer (400 or 500 MHz). The temperature of the measurements was determined by the frequency difference between the two observed peaks for a neat methanol sample[3]. All resonances in the ^{1}H NMR spectra are referenced to the residual solvent peaks (δ 7.16 ppm for benzene, δ 3.58 ppm for THF). Resonances were singlets unless otherwise noted. Line fitting of the resonances in the ^{1}H NMR spectra was performed using MestReNova 10.0.1. Mössbauer data were recorded on a SEECo spectrometer with alternating constant acceleration; isomer shifts are relative to iron metal at 298 K. The sample temperature was maintained at 80 K in a Janis Research Company Inc. cryostat. The zero-field spectra were simulated using Lorentzian doublets using WMoss (SeeCo). Elemental analyses were obtained from the CENTC Elemental Analysis Facility at the University of Rochester. Microanalysis samples were weighed on a PerkinElmer Model AD-6 Autobalance, analyzed on a PerkinElmer 2400 Series II Analyzer and handled in a VAC Atmospheres glovebox under argon.

Complex 3 • $[Na(THF)_3]_2$

A solution of **1** (266.1 mg, 0.50 mmol) in THF (4 mL) was stirred in a cold well at -78 °C (dry ice/acetone) for 15 minutes. A suspension of Na sand (12.9 mg, 0.56 mmol) in THF (2 mL) was added dropwise. The mixture was stirred at ambient temperature for 1 h, then filtered through a plug of Celite. Pentane (6 mL) was added and the mixture was cooled to -40 °C. After 16 h, dark crystals were collected via filtration, washed with pentane and dried under vacuum (127 mg). The mother liquor was dried to give a brown residue, which was extracted with THF (4 mL). The extracts were filtered, pentane was added (5 mL) and the solution was cooled to -40 °C for 2 d to give another crop of dark crystals (122 mg). This process was repeated once more to give a third crop of dark crystals (23 mg). Combined yield: 272 mg, 71 %. ^{1}H NMR (400 MHz, 298 K, THF-d_8): δ 157.6 (2H, p-tol *m*-CH), 115.4 (2H, Ph *o*-CH or p-tol *o*-CH)*, 83.2 (2H, Ph *o*-CH or p-tol *o*-CH)*, 75.2 (2H, p-tol *m*-CH), 37.4 (18H, $SiMe_3$), 14.7 (6H, CH_3), 12.5 (18H , $SiMe_3$), -16.6 (4H, Ph-H), -19.6 (4H, Ph-H), -50.7 (2H, Ph *o*-CH or p-tol *o*-CH)*, -66.7 (2H, Ph *o*-CH or p-tol *o*-CH)*. Tentative peak assignments were based on relative integration, broadness of the resonance (*o*-Ph CH protons broaden due to close proximity to the metal center), chemical shift, and similarity to complexes **1**, **2** and $(formazanate)_2Fe$.[4] *integral deviates from the expected value, presumably due to the broadness of the resonance. Magnetic moment using Evans method (THF-d_8): μ_{eff} = 6.9 ± 0.3 μ_B. Anal. Calcd for $C_{76}H_{118}Fe_2N_{10}Na_2O_6Si_4$ (**3** • $[Na(THF)_3]_2$): C, 59.36; H, 7.73; N, 9.11. Found C, 59.22; H, 7.50; N, 9.44 (~6 equivalents THF were confirmed through integration in the ^{1}H NMR spectrum). Zero-field Mössbauer (80 K): δ = 0.74 mm/s and $|\Delta E_Q|$ = 2.30 mm/s. IR-ATR (cm^{-1}): 3045 (w), 2939 (m), 2876 (m), 1583 (s), 1563 (m), 1511 (w), 1475 (s), 1451 (w), 1415 (m), 1317 (m), 1300 (w), 1256 (m), 1219 (s), 1167 (m), 1156 (m), 1088 (s), 1065 (s), 1049 (s), 975 (s), 916 (w), 863 (s), 834 (s), 817 (s), 781 (s), 749 (s), 711 (m), 685 (s), 658 (s), 613 (m), 590 (m), 516 (m), 504 (s), 470 (w), 453 (w).

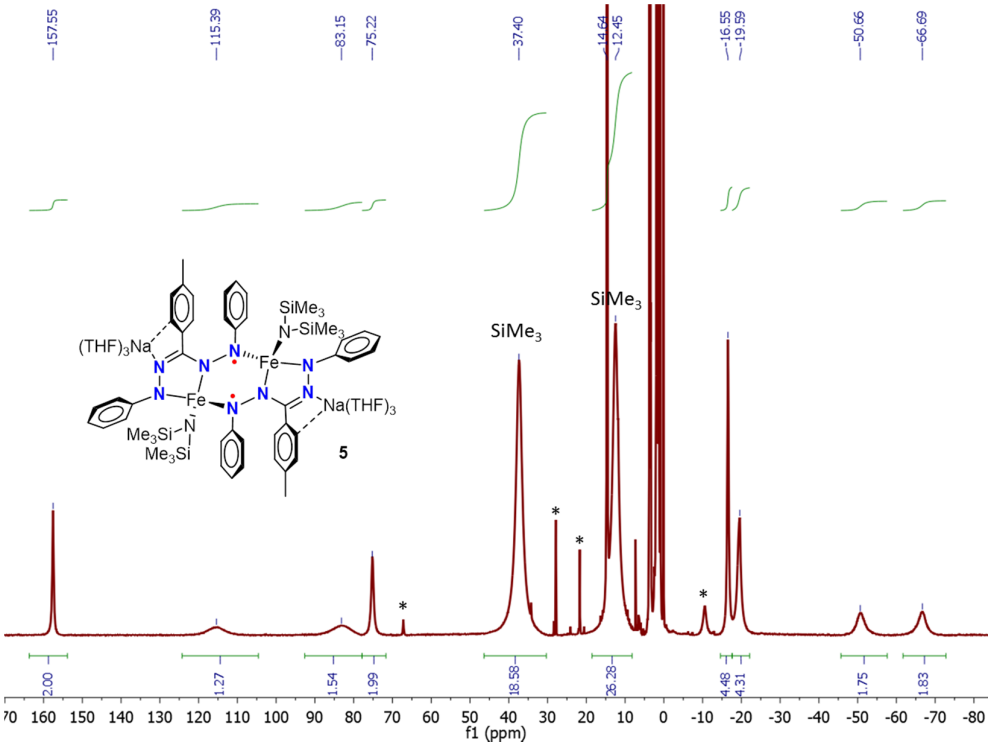

Figure S1. ^{1}H NMR spectrum of complex **3** in THF-d_8. * indicates peaks originating from the partial dissociation of the dimeric complex.

Complex 3 • $[K(THF)]_2$

A solution of **1** (80.1 mg, 0.15 mmol) in THF (1.5 mL) was stirred in a cold well at -78 °C (dry ice/acetone) for 15 minutes. Solid KC_8 (21.7 mg, 0.16 mmol) was added, after which the mixture was removed from the cold well, and was stirred at ambient temperature for 1 h. The dark mixture was filtered through a plug of Celite, mixed with pentane (3 mL) and cooled to -40 °C. After 16 h, dark crystals were collected via filtration, washed with pentane and dried under vacuum (38 mg). The pentane washings were added to the mother liquor and the resulting mixture was placed at -40 °C for 2 d to give an additional crop of dark crystals (36 mg). Repeating the last step gave a third crop of dark crystals (10 mg). Combined yield: 78 mg, 81%. ^{1}H NMR (400 MHz, 283 K, THF-d_8): δ 161.9 (2H, p-tol *m*-CH), 118.8(2+4H, p-tol *m*-CH + Ph *o*-CH or p-tol *o*-CH)*, 37.8 (18H, $SiMe_3$), 14.4 (6H, CH_3), 12.5 (18H, $SiMe_3$), -10.5 (4+4H, Ph-H)*, -51.5 (2H, Ph *o*-CH or p-tol *o*-CH), -68.9 (2H, Ph *o*-CH or p-tol *o*-CH). Tentative peak assignments were based on relative integration, broadness of the resonance (*o*-Ph CH protons broaden due to close proximity to the metal center), chemical shift, and similarity to complexes **1**, **2** and $(formazanate)_2Fe$.[4] *integral deviates from the expected value, presumably due to the broadness of the resonance. Magnetic moment using Evans method (THF-d_8, 283 K): μ_{eff} = 6.9

± 0.3 μ_B. Anal. Calcd for $C_{60}H_{86}Fe_2K_2N_{10}O_2Si_4$ (**3** • $[K(THF)]_2$): C, 56.23; H, 6.76; N, 10.96. Found C, 56.17; H, 6.35; N, 10.96. (~2 equivalents THF were confirmed through integration in the ^{1}H NMR spectrum). Zero-field Mössbauer (80 K): δ = 0.72 mm/s and $|\Delta E_Q|$ = 2.16 mm/s. IR-ATR (cm^{-1}): 3045 (w), 2939 (m), 2876 (m), 1583 (s), 1563 (m), 1511 (w), 1475 (s), 1451 (w), 1420 (m), 1321 (m), 1300 (w), 1219 (s), 1167 (m), 1150 (m), 1088 (s), 1065 (s), 1046 (s), 962 (s), 916 (w), 863 (s), 834 (s), 817 (s), 780 (s), 749 (s), 711 (m), 692 (s), 658 (s), 613 (m), 590 (m), 518 (m), 504 (s), 466 (w), 453 (w).

Complex 3 • $[Rb(THF)]_2$

A solution of **1** (56.1 mg, 0.11 mmol) in THF (1.0 mL) was stirred in a cold well at -78 °C (dry ice/acetone) for 15 minutes. Solid RbC_8 (20.0 mg, 0.11 mmol) was added, after which the mixture was removed from the cold well, and was stirred at ambient temperature for 1 h. The dark mixture was filtered through a plug of Celite, mixed with pentane (2 mL) and cooled to -40 °C. After 16 h, crystals were collected via filtration, washed with pentane and dried under vacuum (30 mg). The pentane washings were added to the mother liquor and the resulting mixture was placed at -40 °C for 2 d to give an additional crop of dark crystals (20 mg). Repeating the last step gave a third crop of dark crystals (9 mg). Combined yield: 59 mg, 79%. ^{1}H NMR (400 MHz, 283 K, THF-d_8): δ 153.2 (2H, p-tol *m*-CH), 124.4 (2H, p-tol *m*-CH), 37.4 (18H, $SiMe_3$)*, 13.5 (6H, CH_3), 12.5 (18H, $SiMe_3$)*, -18.6 (4+4H, Ph-H), -21.6 (4H) -49.1 (2H, Ph *o*-CH or p-tol *o*-CH)*, -65.8 (2H, Ph *o*-CH or p-tol *o*-CH)*. Tentative peak assignments were based on relative integration, broadness of the resonance (*o*-Ph CH protons broaden due to close proximity to the metal center), chemical shift, and similarity to complexes **1**, **2** and $(formazanate)_2Fe$.[4] *integral deviates from the expected value, presumably due to the broadness of the resonance. Magnetic moment using Evans method (THF-d_8, 283 K): μ_{eff} = 7.0 ± 0.3 μ_B. Anal. Calcd for $C_{60}H_{86}Fe_2Rb_2N_{10}O_2Si_4$ (**3** • $[Rb(THF)]_2$): C, 52.44; H, 6.31; N, 10.19. Found C, 51.73; H, 5.97; N, 10.42. (~2 equivalents THF were confirmed through integration in the ^{1}H NMR spectrum). Zero-field Mössbauer (80 K): δ = 0.71 mm/s and $|\Delta E_Q|$ = 2.17 mm/s. IR-ATR (cm^{-1}): 3045 (w), 2939 (m), 2876 (m), 1580 (s), 1563 (m), 1511 (w), 1475 (s), 1451 (w), 1415 (m), 1321 (m), 1300 (w), 1219 (s), 1167 (m), 1149 (m), 1088 (s), 1061 (s), 1049 (s), 975 (s), 910 (w), 863 (s), 834 (s), 817 (s), 781 (s), 749 (s), 713 (m), 690 (s), 662 (s), 613 (m), 590 (m), 518 (m), 504 (s), 467 (w), 453 (w).

Complex 3 • $[Cs(THF)_{0.5}]_2$

A solution of **1** (52.1 mg, 0.10 mmol) in THF (1.0 mL) was stirred in a cold well at -78 °C (dry ice/acetone) for 15 minutes. Solid CsC_8 (23.8 mg, 0.10 mmol) was added, after which the mixture was removed from the cold well, and was stirred at ambient temperature for 1 h. The dark mixture was filtered through a plug of Celite, mixed with pentane (2 mL) and cooled to -40 °C. After 16 h, dark crystals were collected via filtration, washed with pentane and dried under vacuum (14 mg). The pentane washings were added to the mother liquor and the resulting mixture was placed at -40 °C for 2 d to give an additional crop of dark crystals (31 mg). Repeating the last step gave a third crop of dark crystals (8 mg). Combined yield: 53 mg, 77%. ^{1}H NMR (400 MHz, 283 K, THF-d_8): δ 140.9 (2H, p-tol *m*-CH), 129.0 (2H, p-tol *m*-CH), 112.3 (2H, Ph *o*-CH or p-tol *o*-CH)*, 98.0 (2H, Ph *o*-CH or p-tol *o*-CH), 36.8 (18H, $SiMe_3$)*, 12.6 (18H, $SiMe_3$), 11.8 (6H, CH_3), -17.4 (4H, Ph-H), -21.6 (4H, Ph-H) -45.4 (2H, Ph *o*-CH or p-tol *o*-CH)*, -60.8 (2H, Ph *o*-CH or p-tol *o*-CH)*. Tentative peak assignments were based on relative integration, broadness of the resonance (*o*-Ph CH protons broaden due to close proximity to the metal center), chemical shift, and similarity to complexes **1**, **2** and $(formazanate)_2Fe$.[4] *integral deviates from the expected value, presumably due to the broadness of the resonance. Magnetic moment using Evans method (THF-d_8, 283 K): $\mu_{eff} = 6.7 \pm 0.3\ \mu_B$. Anal. Calcd for $C_{56}H_{78}Fe_2Cs_2N_{10}OSi_4$ (**3** • $[Cs(THF)_{0.5}]_2$): C, 48.15; H, 5.63; N, 10.03. Found C, 48.19; H, 5.37; N, 10.16. (~1 equivalent of THF was confirmed through integration in the ^{1}H NMR spectrum). Zero-field Mössbauer (80 K): δ = 0.72 mm/s and $|\Delta E_Q| = 2.18$ mm/s. IR-ATR (cm^{-1}): 3045 (w), 2939 (m), 2876 (m), 1583 (s), 1563 (m), 1511 (w), 1475 (s), 1451 (w), 1415 (m), 1317 (m), 1300 (w), 1215 (s), 1167 (m), 1152 (m), 1088 (s), 1060 (s), 1048 (s), 961 (s), 916 (w), 863 (s), 834 (s), 817 (s), 781 (s), 749 (s), 711 (m), 691 (s), 658 (s), 613 (m), 590 (m), 517 (m), 504 (s), 468 (w), 453 (w).

Monomeric complexes 4-Na, **4-K**, **4-Rb** and **4-Cs**

Dimeric complexes **3** and **5-7** in THF-d_8 solution fully convert to the corresponding monomeric species in time.

4-Na: ^{1}H NMR (400 MHz, 298 K, THF-d_8): δ 102.1 (4H, Ph *o*-CH)*, 67.3 (2H, p-tol *m*-CH), 27.9 (3H, CH_3), 21.7 (2H, p-tol *o*-CH), 11.7 (4H, Ph, *m*-CH), -10.5 (18H, $SiMe_3$)*, -19.5 (2H, Ph *p*-CH). *integral deviates from the expected value, presumably due to the broadness of the resonance.

4-K: ^{1}H NMR (400 MHz, 298 K, THF-d_8): δ 99.3 (4H, Ph *o*-CH)*, 65.1 (2H, p-tol *m*-CH), 27.1 (3H, CH_3), 21.2 (2H, p-tol *o*-CH), 11.5 (4H, Ph, *m*-CH), -9.1 (18H, $SiMe_3$)*, -17.5 (2H, Ph *p*-CH). *integral deviates from the expected value, presumably due to the broadness of the resonance.

4-Rb: ^{1}H NMR (400 MHz, 298 K, THF-d_8): δ 95.2 (4H, Ph *o*-CH)*, 60.9 (2H, p-tol *m*-CH), 26.7 (3H, CH_3), 20.9 (2H, p-tol *o*-CH), 12.3 (4H, Ph, *m*-CH), -9.1 (18H, $SiMe_3$)*, -18.5 (2H, Ph *p*-CH). *integral deviates from the expected value, presumably due to the broadness of the resonance.

4-Cs: ^{1}H NMR (400 MHz, 298 K, THF-d_8): δ 85.3 (4H, Ph *o*-CH)*, 52.4 (2H, p-tol *m*-CH), 25.8 (3H, CH_3), 20.5 (2H, p-tol *o*-CH), 14.5 (4H, Ph, *m*-CH), -7.8 (18H, $SiMe_3$)*, -15.7 (2H, Ph *p*-CH). *integral deviates from the expected value, presumably due to the broadness of the resonance.

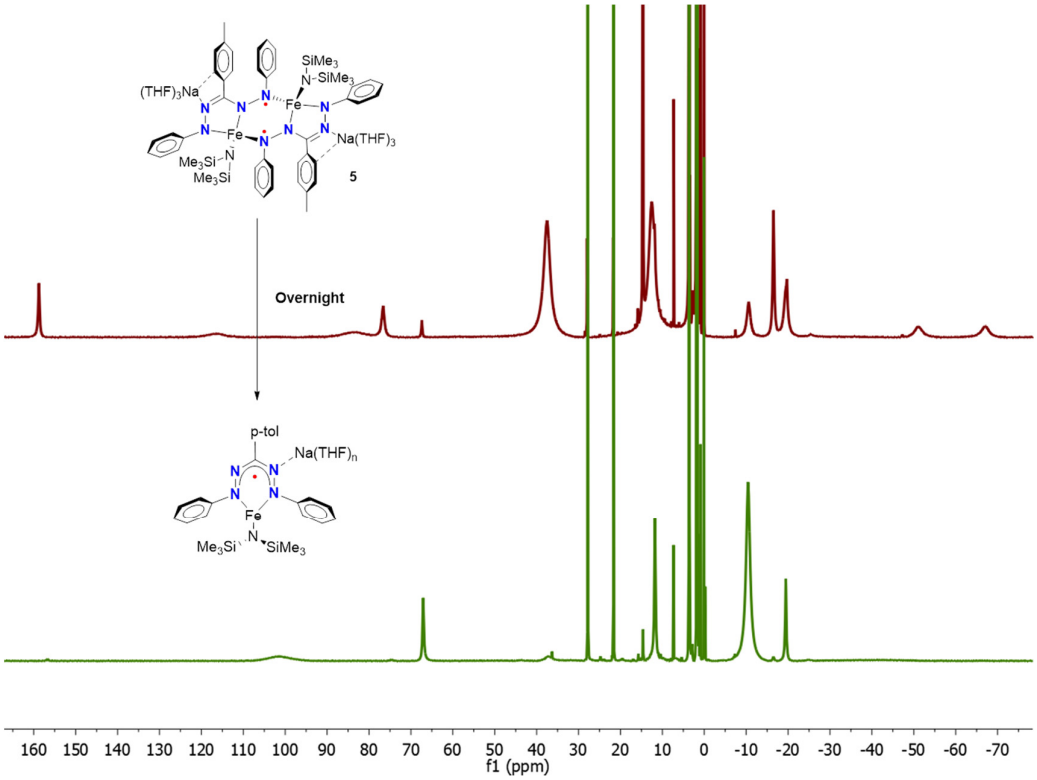

Figure S2. Stacked ^{1}H NMR spectra of complex **3-Na** (top) and of the same solution the next day (**4-Na**, bottom).

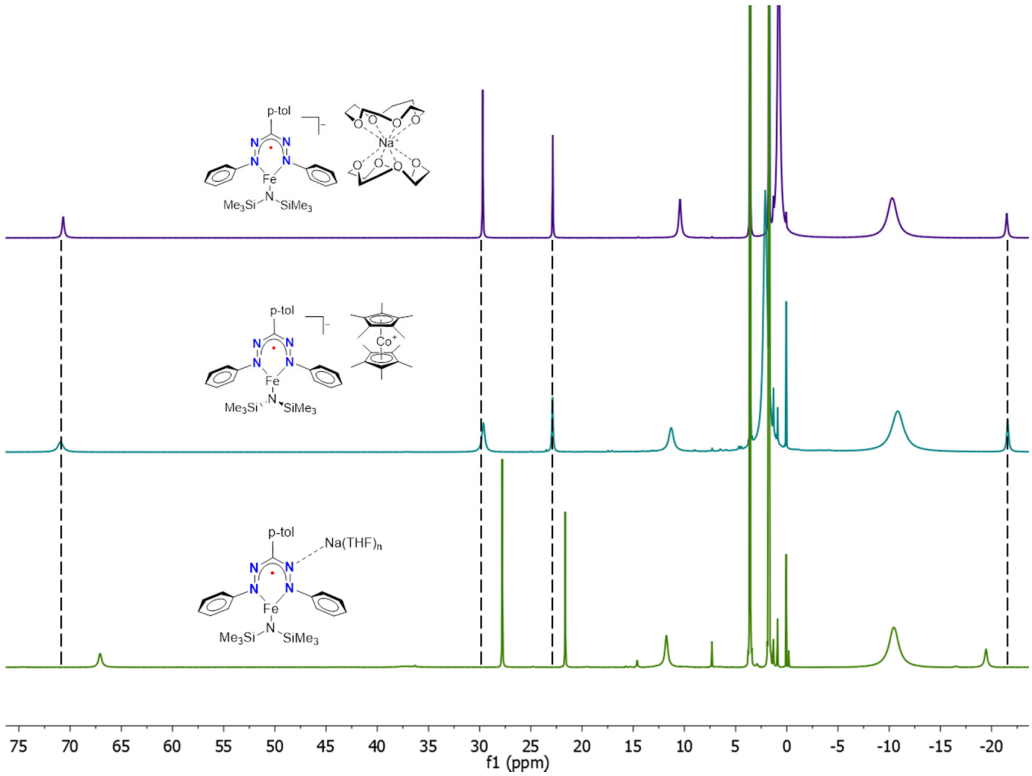

Figure S3. Stacked ^{1}H NMR spectra of **2** (top), **2[CoCp*$_2$]** (middle), and dissociated **4-Na** in THF-d_8.

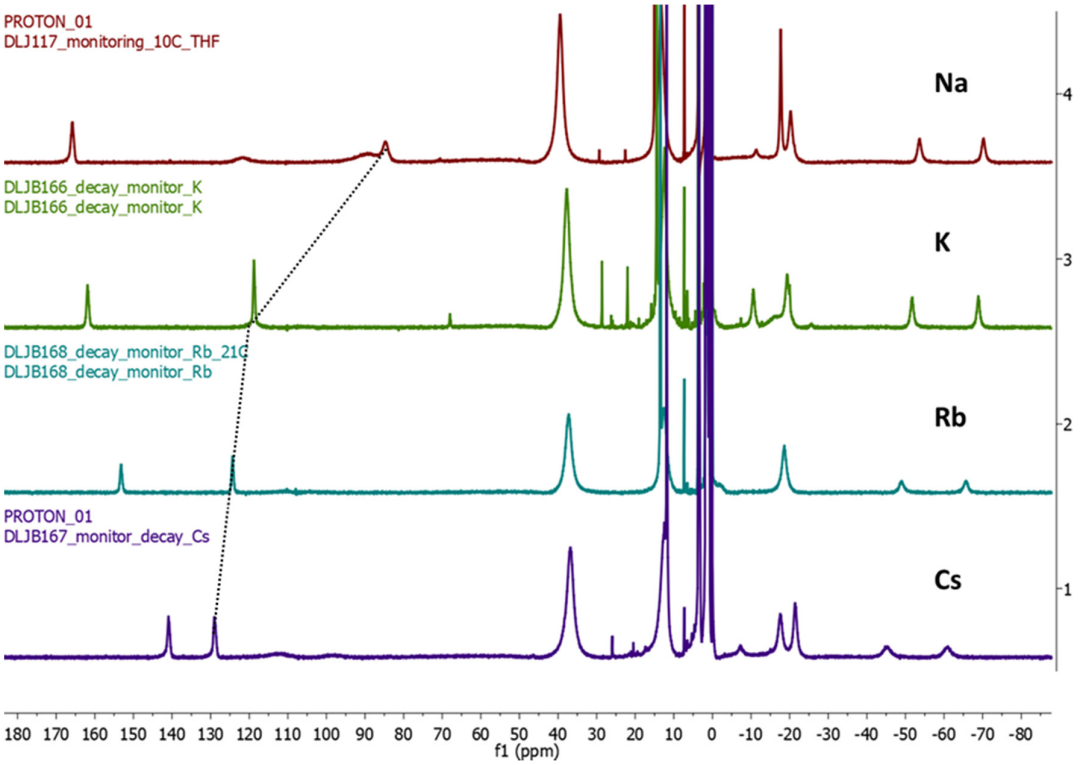

Figure S4. Stacked ^{1}H NMR spectra of the complexes **3** at 10 °C, highlighted a line to show that the Na dimer does not fit the trend for all chemical shifts.

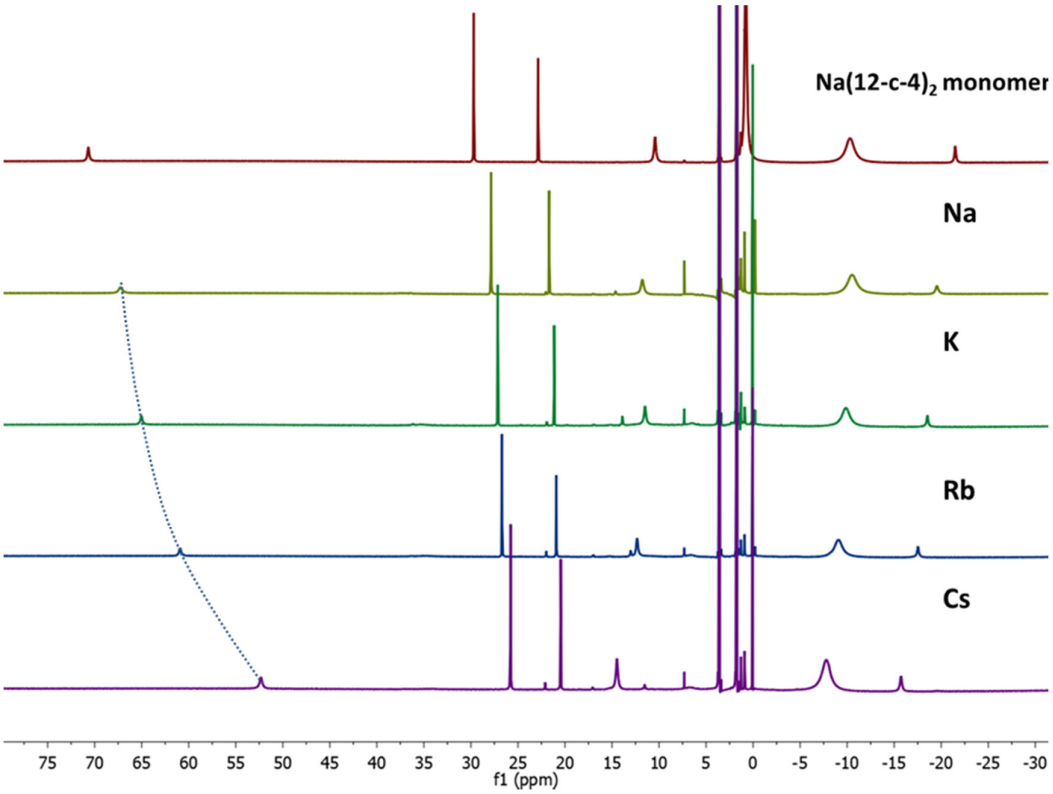

Figure S5. Stacked ^{1}H NMR spectra of complex **2** (top) and dissociated dimeric complexes (**4**), showing the trends in chemical shifts upon binding of alkali cations.

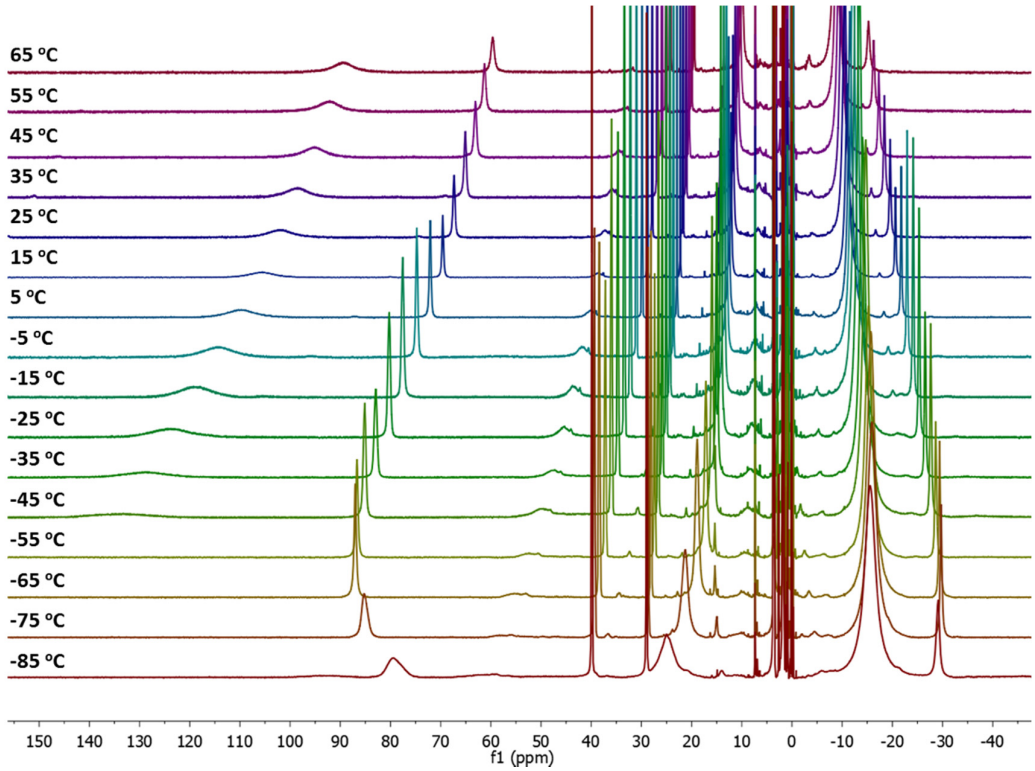

Figure S6. Stacked ^{1}H NMR spectra of **4-Na** in THF-d_8 between 65 and -85 °C.

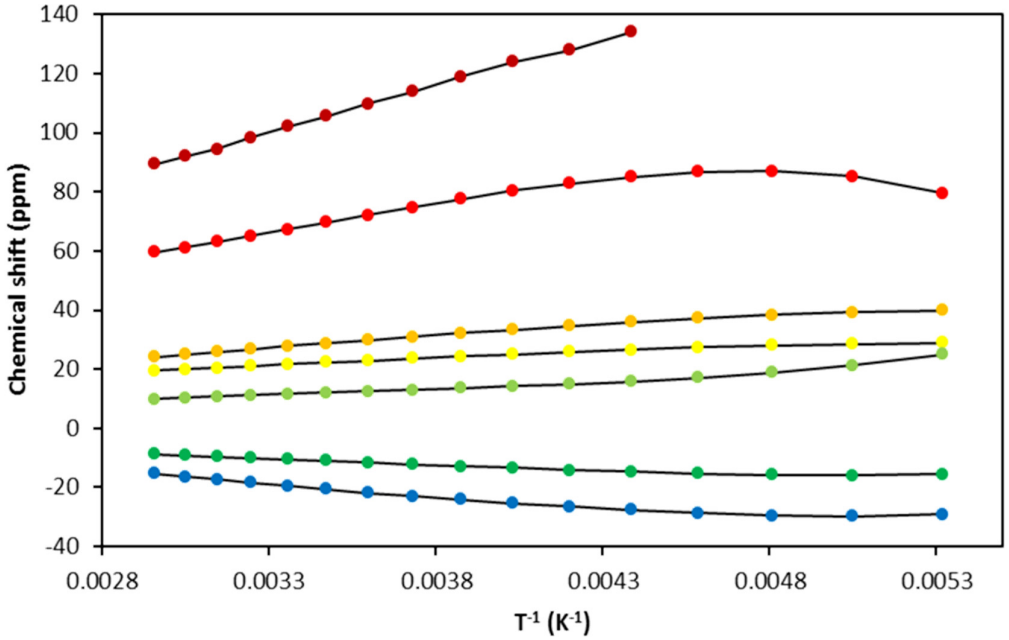

Figure S7. Curie plot obtained from the VT NMR measurements of dissociated **4-Na**.

Mössbauer spectra of dimers (3)

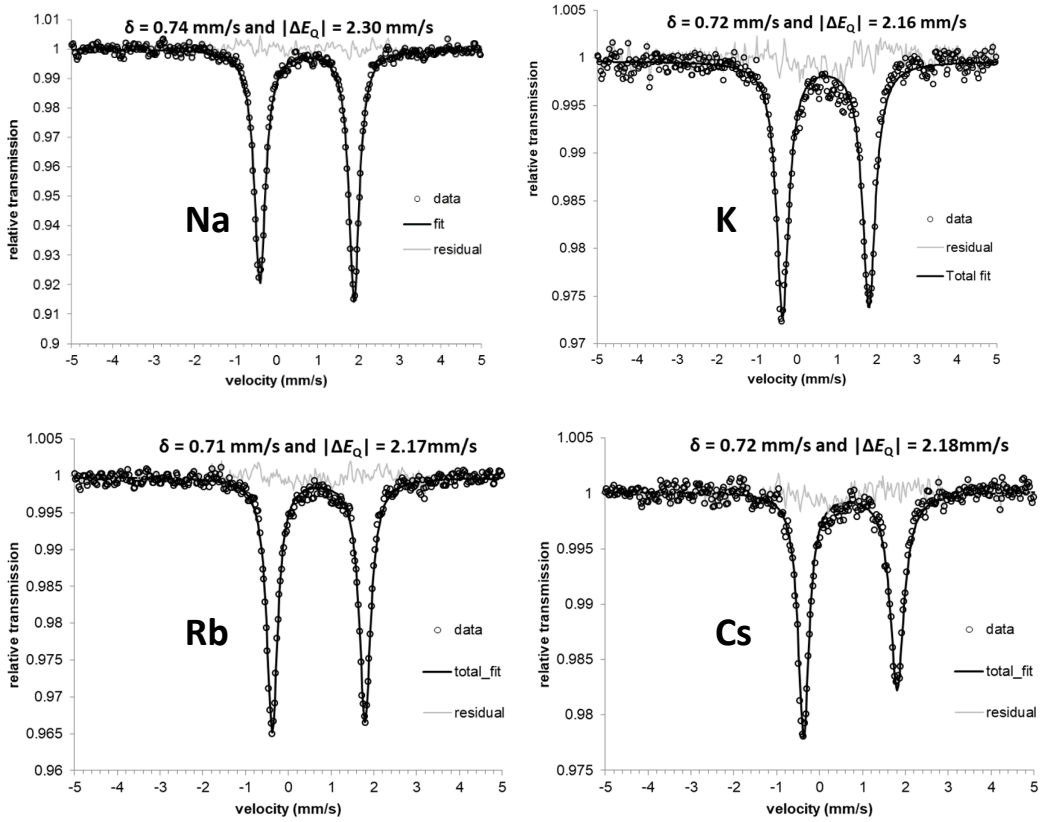

Figure S8. Mössbauer spectra of dimers **3-Na** (top left), **3-K** (top right), **3-Rb** (bottom left) and **3-Cs** (bottom right), with the samples held at 80 K.

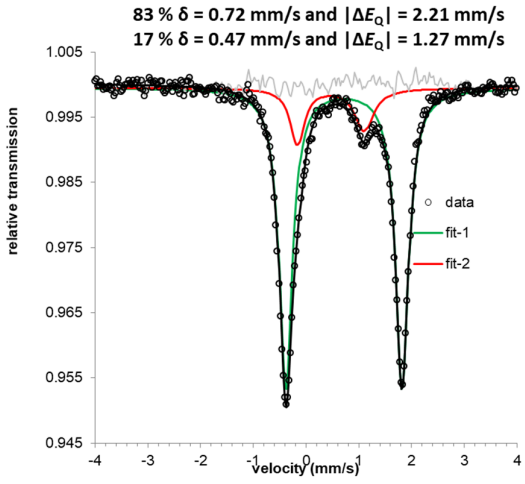

Figure S9. Mössbauer spectrum (80 K) of the crystalline material obtained when dimer **3-K** is rapidly crystallized from a THF/hexane mixture. The major component (fit-1) corresponds to **3-K** and the minor component (fit-2) corresponds to monomeric **4-K**.

Determination of activation parameters for the conversion of 3-Na into 4-Na

Solutions of **3-Na** (7.0 x 10^{-3} M) were made inside a N_2 filled glovebox using cold THF, placed in a J. Young NMR tube and transported cold to the NMR spectrometer to prevent dissociation into the dimer. The NMR tube was subsequently placed in the NMR spectrometer at the preset temperature after which spectra were recorded at regular intervals to monitor [dimer] through integration of the well separated $SiMe_3$ resonances. Curve fitting of the decay curves using Eq. 1 afforded rate constants, which were used to generate an Eyring plot with slope = $\Delta H^{\ddagger}/R$ and intercept = $\ln(k_B/h) + (\Delta S^{\ddagger}/R)$ where R is the gas constant, k_B is Boltzmann constant, and h is Planck's constant. The activation parameters were determined as $\Delta H^{\ddagger}$ = 28.0 ± 1.1 kcal mol^{-1} and $\Delta S^{\ddagger}$ = -17.4 ± 3.7 cal mol^{-1} K^{-1} The same values within error ($\Delta H^{\ddagger}$ = 27.4 ± 1.6 kcal mol^{-1} and $\Delta S^{\ddagger}$ = -14.9 ± 5.6 cal mol^{-1} K^{-1}) were obtained from an Eyring plot (Figure S16) that was generated using rate constants obtained from the slope of plots of ln[dimer] vs time (Figure S10-S15). Uncertainties in the rate constants are standard errors determined from curve fitting using Kaleidagraph (4.5.0). The uncertainties in the activation parameters were determined by propagation of the errors obtained from linear regression in the Eyring plot.

$$[\text{dimer}]_t - [\text{dimer}]_{final} = [\text{dimer}]_0 e^{-kt} \qquad \text{Eq. 1}$$

Table S1. Rate constants obtained from curve fitting.

Temperature (K)	***k***
273	1.32 ± 4.71 x 10^{-6}*
283	1.12 ± 0.06 x 10^{-5}
294	8.53 ± 0.15 x 10^{-5}
303	2.69 ± 0.04 x 10^{-4}
313	1.14 ± 0.01 x 10^{-5}

* This value has a large uncertainty because at this temperature (273 K) we could not monitor the reaction for multiple half-lives, which reduced the quality of the fit.

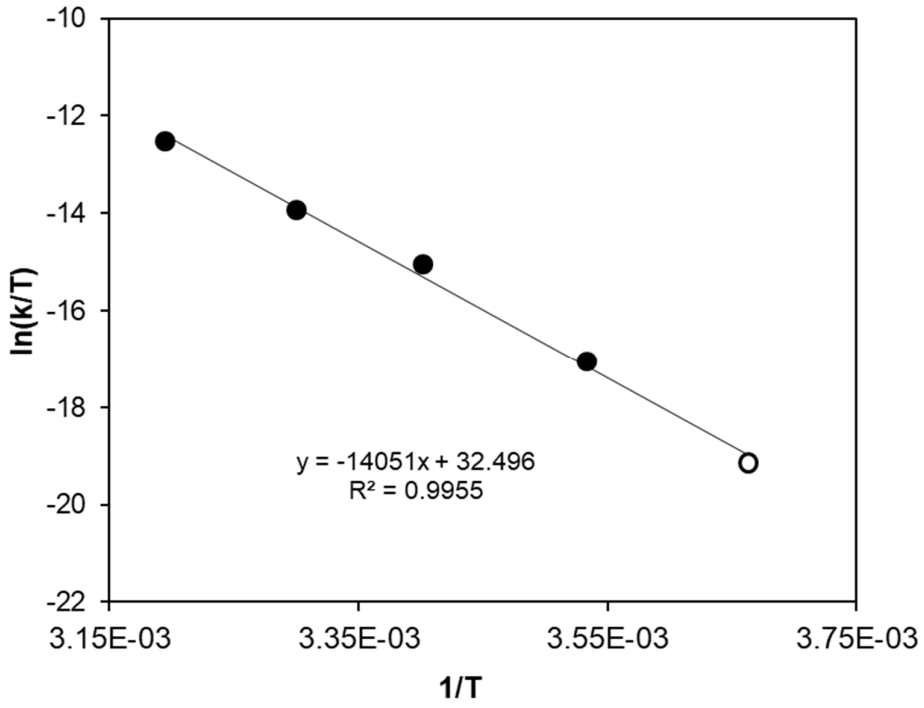

Figure S10. Eyring plot for the dissociation of complex **3-Na** in THF solution into a mononuclear species with values for *k* obtained from curve fitting. The hollow data point has a large error because at this temperature (273 K) we could not monitor the reaction for multiple half-lives, affecting the quality of the fit. Omitting this data point from the linear regression gives activation parameters within the error margins of the values that are obtained when it is included.

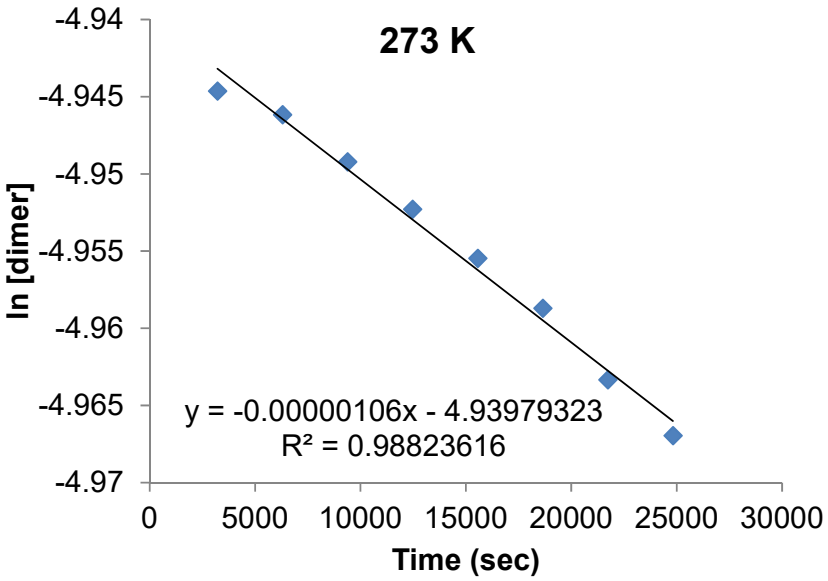

Figure S11. Plot of ln[dimer] vs time at 273 K showing a 1st order decay.

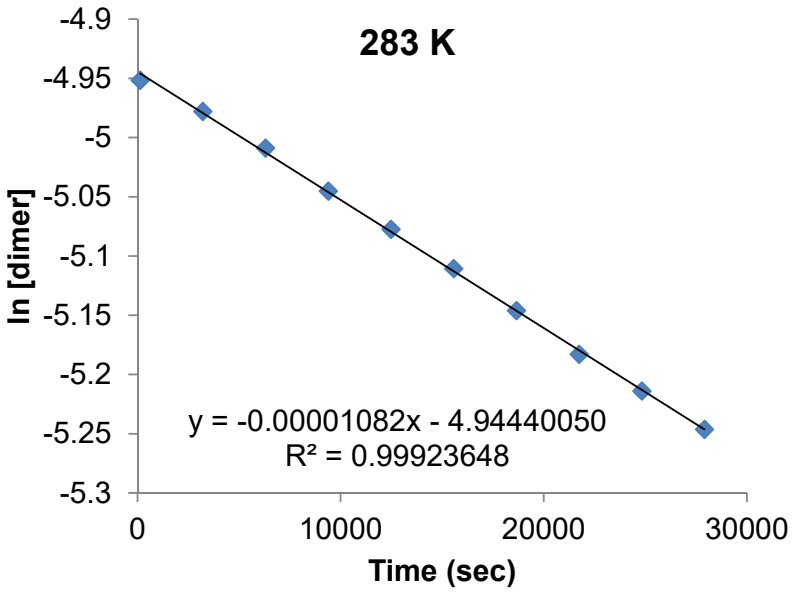

Figure S12. Plot of ln[dimer] vs time at 283 K showing a 1st order decay.

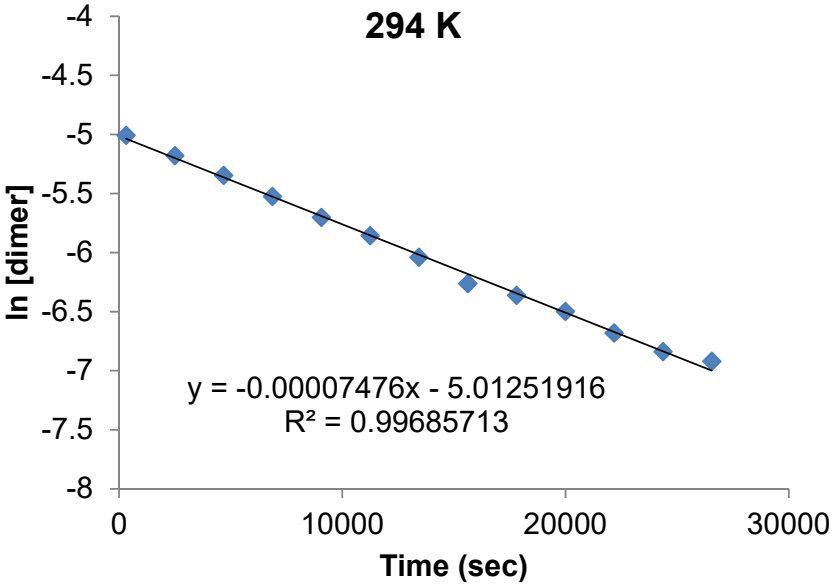

Figure S13. Plot of ln[dimer] vs time at 294 K showing a 1st order decay.

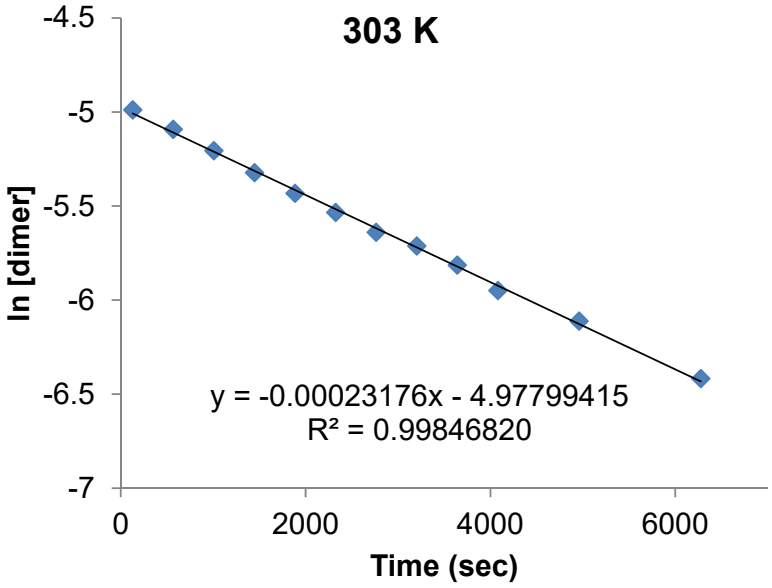

Figure S14. Plot of ln[dimer] vs time at 303 K showing a 1st order decay.

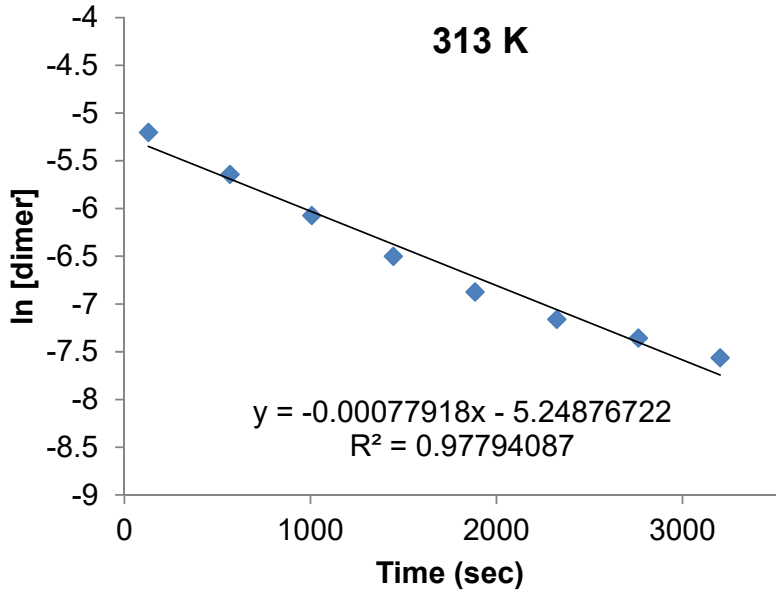

Figure S15. Plot of ln[dimer] vs time at 313 K showing a 1st order decay.

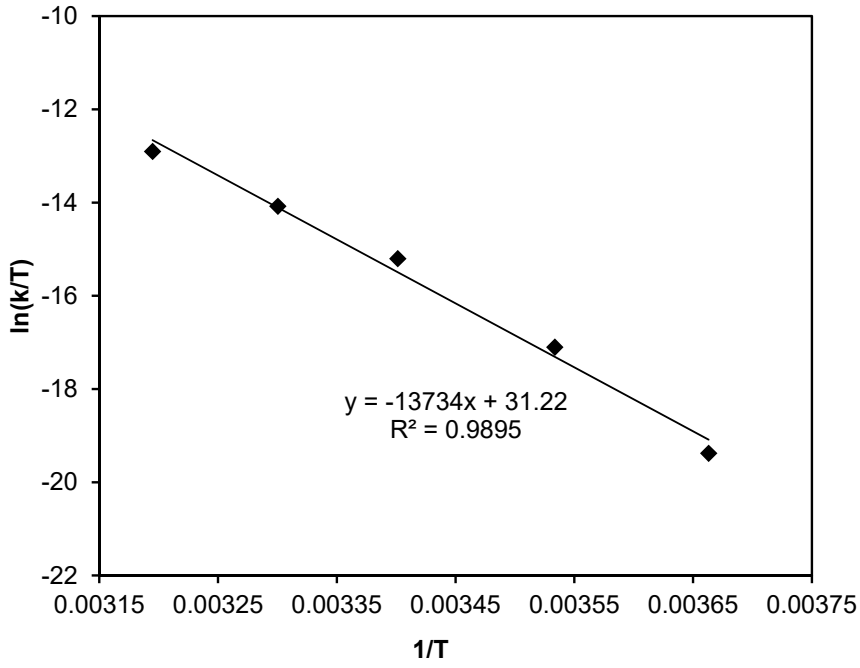

Figure S16. Eyring plot for the dissociation of complex **3-Na** in THF solution into a mononuclear species with values for *k* obtained from curve fitting.

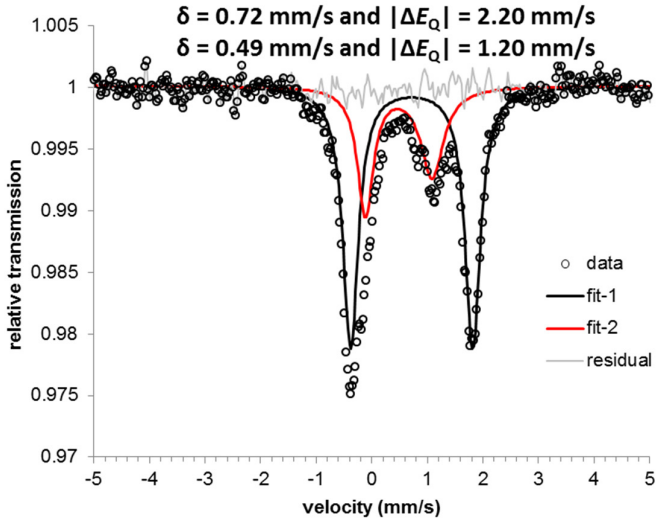

Figure S17.Mössbauer spectrum of a THF solution containing partially dissociated **3-Na/4-Na**.

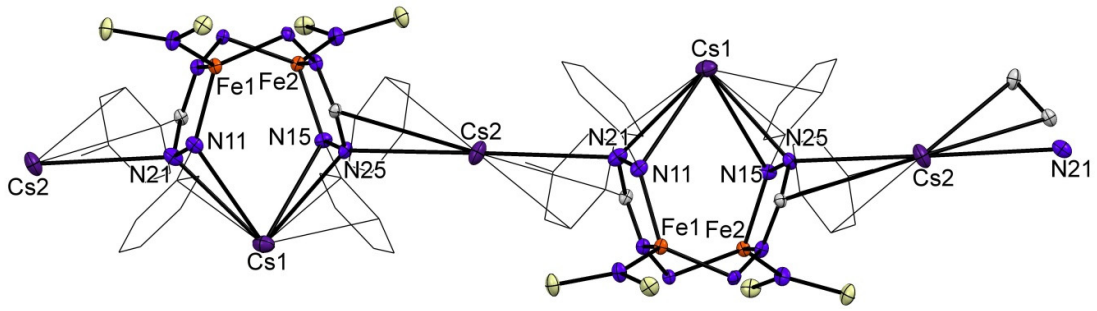

Figure S18. Displacement ellipsoid plot (50% probability) of complex **3-Cs** showing the repeating polymeric structure.

X-ray Absorption Spectroscopy

Fe K-edge data were collected on the 16 pole, 2 T wiggler beamline 9-3 at the Stanford Synchrotron Radiation Lightsource (SSRL) under ring conditions of 3 GeV and 500 mA. Samples were diluted in BN, pressed into a 1 mm aluminium spacer and sealed with 37 μm Kapton tape. A Si(220) double-crystal monochromator was used for energy selection and a Rh-coated mirror (set to an energy cutoff of 9 keV) was used for harmonic rejection. Internal energy calibration was performed by assigning the first inflection point of a Fe foil spectrum to 7111.2 eV. Data were collected in transmission mode using N_2-filled ionization chambers with the sample maintained at 10 K in a liquid helium flow cryostat. Data represent the average of 4 scans. Data were processed using the MAVE and PROCESS modules of the EXAFSPAK software package,[5] by fitting a second-order polynomial to the pre-edge region and subtracting this background from the entire spectrum. A three-region cubic spline was used to model the smooth background above the edge. The absorbance was normalized by subtracting the spline and normalizing the postedge absorbance to 1.0.

Temperature dependence of μ_{eff} (T) for 3-Na

SQUID measurements of a solid sample of **3-Na** in the temperature range 50–300 K showed a magnetic moment (μ_{eff}) of 7.6 μ_{B}. (Figure S19). The result is notably close to the spin-only (s.o.) value for four essentially uncoupled spins, i.e. two $S_{\mathrm{Fe},i} = 2$ and two radicals $S_{\mathrm{rad},j} = {}^1/_2$, namely $\mu_{\mathrm{eff,\,s.o.}} = g_e\sqrt{[2(2+1) + 2(2+1) + {}^1/_2({}^1/_2+1) + {}^1/_2({}^1/_2+1)]} = 7.3\ \mu_{\mathrm{B}}$. The temperature independence of μ_{eff}(T) in this temperature range provides limits for the various pair exchange coupling constants $|J_{ij}|$ between the four spins in the system of less than a few wavenumbers (Figure S19). Estimates were obtained from explorations of the possible parameter space by single-point simulations. Unfortunately, exact *J*-value cannot be provided, neither zero-field splitting parameters for iron(II), because the low-temperature magnetic data are severely obscured by steep over-shooting of μ_{eff}(T) below 50 K due to intermolecular interaction. The preliminary fits suggest at most moderate zero-field splitting for iron, the iron-radical coupling should be $|J_{\mathrm{Fe\text{-}rad}}| < 5\ \mathrm{cm}^{-1}$ ($\hat{H}_{\mathrm{ex}} = -2J\, S_1 \cdot S_2$), and the iron *g*-values is close to 2, $g_{Fe} = 2.07$, adopting $g_{\mathrm{rad}} = g_e$ for the radicals. Both features suggest an orbital non-degenerate ground state for iron(II), which seems to be compatible with the d^6 high-spin configuration in distorted quasi-tetrahedral symmetry (in contrast to compounds **1** and **2**).

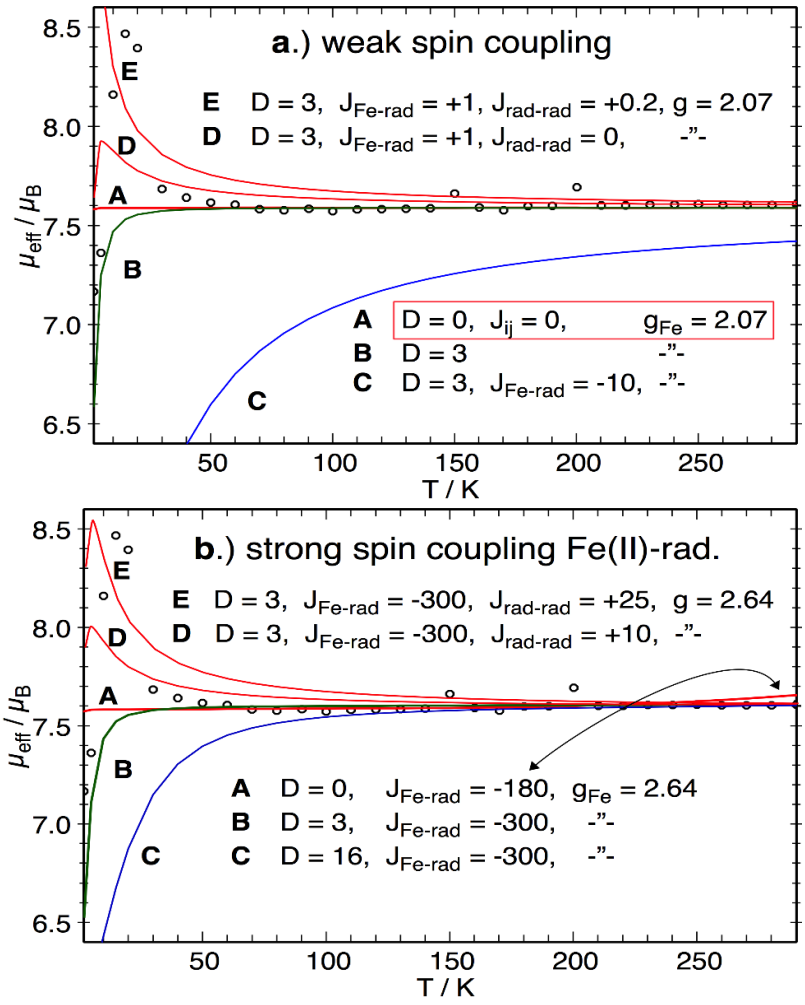

Figure S19. Temperature dependence of effective magnetic moment μ_{eff} (T) for **3-Na** obtained with a polycrystalline sample in 0.1 T external field (dots, same in top and bottom panel). The solid lines represent simulations for a symmetric group of two iron(II), $S_{\text{Fe}} = 2$, coupled to two coordinated ligand radicals with $S_{\text{rad}} = {}^1/_2$, using the following spin Hamiltonian:

$$\hat{H} = -2J_{Fe-rad}\left[\hat{\vec{S}}_{Fe1}\cdot\hat{\vec{S}}_{rad1} + \hat{\vec{S}}_{Fe2}\cdot\hat{\vec{S}}_{rad2}\right] - 2J_{rad}\left[\hat{\vec{S}}_{rad1}\cdot\hat{\vec{S}}_{rad2}\right] + g_{Fe}\mu_B\vec{B}\cdot\left(\hat{\vec{S}}_{Fe1} + \hat{\vec{S}}_{Fe2}\right) + g_e\mu_B\vec{B}\cdot\left(\hat{\vec{S}}_{rad1} + \hat{\vec{S}}_{rad2}\right) + D_{Fe}\left[\hat{S}^2_{Fe1,z} + \hat{S}^2_{Fe1,z} - 12\right]$$

The high temperature data above 50 K can be simulated with four uncoupled or weakly coupled spins (yielding $g_{\text{Fe}} = 2.073$, curve A, top), as well as with strong Fe-radical coupling, $-J_{\text{Fe-rad}} > 300$ cm^{-1} (yielding $g_{\text{Fe}} = 2.64$, bottom). In an alternative fit, the lower limit for Fe-radical coupling is $|J_{\text{Fe-rad}}| = 180$ cm^{-1} (curve A, bottom). Spin Hamiltonian parameters are given in the inset (in cm^{-1}); g_{rad} was fixed to 2. The experimental data are corrected for diamagnetism, $\chi_{\text{dia}} = -769 \times 10^{-6}$ cm^3 mol^{-1}. The peak of μ_{eff}(T) below 30 K is too steep to be simulated by any choice of J in a spin tetramer. We assign the peak to a weak intermolecular interaction.

X-ray Crystallography

Cryo-mounting of crystals

A glass slide with a drop of Fomblin immersion oil, a sealable 100 mL vial, and a spatula were cooled in a glovebox cold well at -78 °C (dry ice/acetone). With the cold spatula coated immersion oil, crystalline material was scooped directly from a vial containing the crystals and mother liquor, and transferred onto the immersion oil on the cold slide. The slide was transferred into the precooled 100 mL vial, and transported on dry ice to a microscope equipped with a cold stream (-80 °C). A crystal was selected, mounted on a loop, placed in a cold cryo-pin tong, transported in liquid N_2 and mounted on the diffractometer under a cold stream -180 °C.

3-Na

Low-temperature diffraction data (ω-scans) were collected on a Rigaku MicroMax-007HF diffractometer coupled to a Saturn994+ CCD detector with Cu Kα (λ = 1.54178 Å) for the structure of **3-Na**. The diffraction images were processed and scaled using the Rigaku CrystalClear software (CrystalClear and CrystalStructure; Rigaku/MSC: The Woodlands, TX, 2005). The structure was solved with SHELXT and was refined against F^2 on all data by full-matrix least squares with SHELXL (Sheldrick, G. M. Acta Cryst. 2008, A64, 112–122). All non-hydrogen atoms were refined anisotropically. Hydrogen atoms were included in the model at geometrically calculated positions and refined using a riding model. The isotropic displacement parameters of all hydrogen atoms were fixed to 1.2 times the U value of the atoms to which they are linked (1.5 times for methyl groups). The THF solvent molecule is likely disordered, however their positions are nearly overlapping, and additional parameters did not improve the overall refinement metrics of this model. The atoms of the THF (O1A, C1A, C2A, C3A, C4A) were refined with the aid of rigid bond restraints, as the atoms of the solvent were anticipated to have similar tensor directions. Additionally, reflection (2 1 4) was improperly recorded and subsequently omitted. The full numbering scheme of compound **3-Na** can be found in the full details of the X-ray structure determination (CIF), which is included as Supporting Information. CCDC number 1815890 (**3-Na**) contains the supplementary crystallographic data for this paper. These data can be obtained free of charge from The Cambridge Crystallographic Data Center via www.ccdc.cam.ac.uk/data_request/cif.

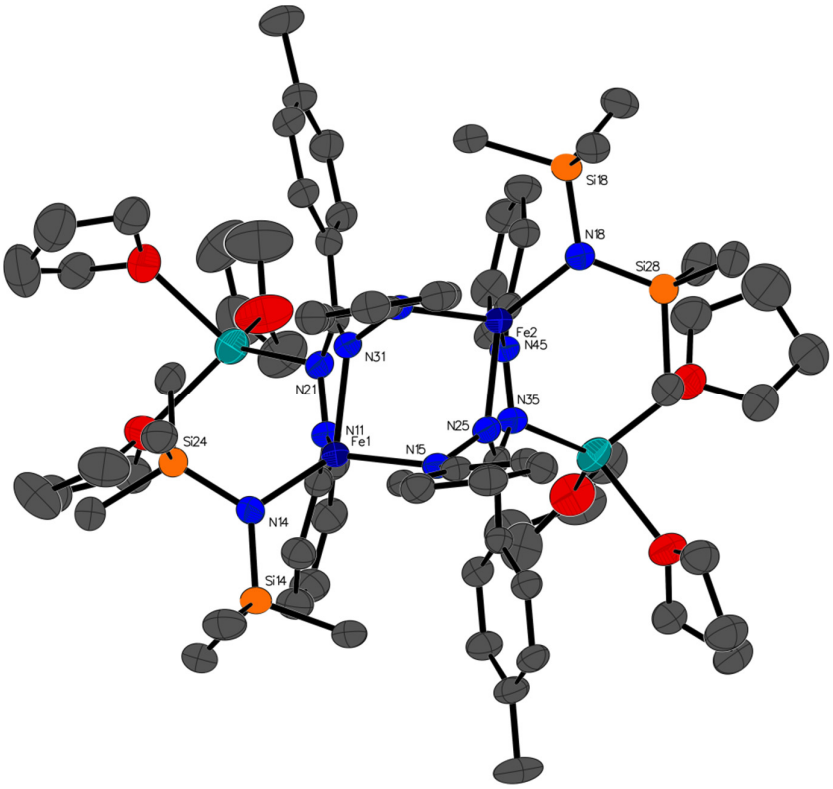

Figure S20. A partial numbering scheme of **3-Na** with 50% thermal ellipsoid probability levels. The hydrogen atoms have been omitted for clarity.

Table S2. Crystal data and structure refinement for **3-Na**.

Identification code	007-16187	
Empirical formula	C80 H126 Fe2 N10 Na2 O7 Si4	
Formula weight	1609.94	
Temperature	93(2) K	
Wavelength	1.54178 Å	
Crystal system	Monoclinic	
Space group	$P2_1/c$	
Unit cell dimensions	a = 20.9709(15) Å	α= 90°.
	b = 19.2848(13) Å	β= 95.9840(10)°.
	c = 21.7285(15) Å	γ = 90°.
Volume	8739.5(10) $Å^3$	
Z	4	
Density (calculated)	1.224 g/cm^3	
Absorption coefficient	3.721 mm^{-1}	
F(000)	3448	
Crystal size	0.080 x 0.050 x 0.030 mm^3	
Theta range for data collection	3.121 to 66.592°.	
Index ranges	-24<=h<=24, -22<=k<=22, -25<=l<=25	
Reflections collected	308721	
Independent reflections	15413 [R(int) = 0.1397]	
Completeness to theta = 66.592°	100.0 %	
Absorption correction	Semi-empirical from equivalents	
Max. and min. transmission	1.000 and 0.860	
Refinement method	Full-matrix least-squares on F^2	
Data / restraints / parameters	15413 / 30 / 960	
Goodness-of-fit on F^2	1.047	
Final R indices [I>2sigma(I)]	R1 = 0.0540, wR2 = 0.1311	
R indices (all data)	R1 = 0.0934, wR2 = 0.1528	
Largest diff. peak and hole	0.805 and -0.613 $e.Å^{-3}$	

4-K

Low-temperature diffraction data (ω-scans) were collected on a Rigaku MicroMax-007HF diffractometer coupled to a Dectris Pilatus3R detector with Mo Kα (λ = 0.71073 Å) for the structure of **4-K**. The diffraction images were processed and scaled using Rigaku Oxford Diffraction software (CrysAlisPro; Rigaku OD: The Woodlands, TX, 2015). The structure was solved with SHELXT and was refined against F^2 on all data by full-matrix least squares with SHELXL (Sheldrick, G. M. Acta Cryst. 2008, A64, 112–122). All non-hydrogen atoms were refined anisotropically. Hydrogen atoms were included in the model at geometrically calculated positions and refined using a riding model. The isotropic displacement parameters of all hydrogen atoms were fixed to 1.2 times the U value of the atoms to which they are linked (1.5 times for methyl groups). One carbon atom in one of the four THF molecules is disordered over two, equally occupied sites. No additional restraints were required and the hydrogen atoms were placed as riding atoms to reflect the disordered positions. The full numbering scheme of compound **4-K** can be found in the full details of the X-ray structure determination (CIF), which is included as Supporting Information. CCDC number 1815888 (**4-K**) contains the supplementary crystallographic data for this paper. These data can be obtained free of charge from The Cambridge Crystallographic Data Center via www.ccdc.cam.ac.uk/data_request/cif.

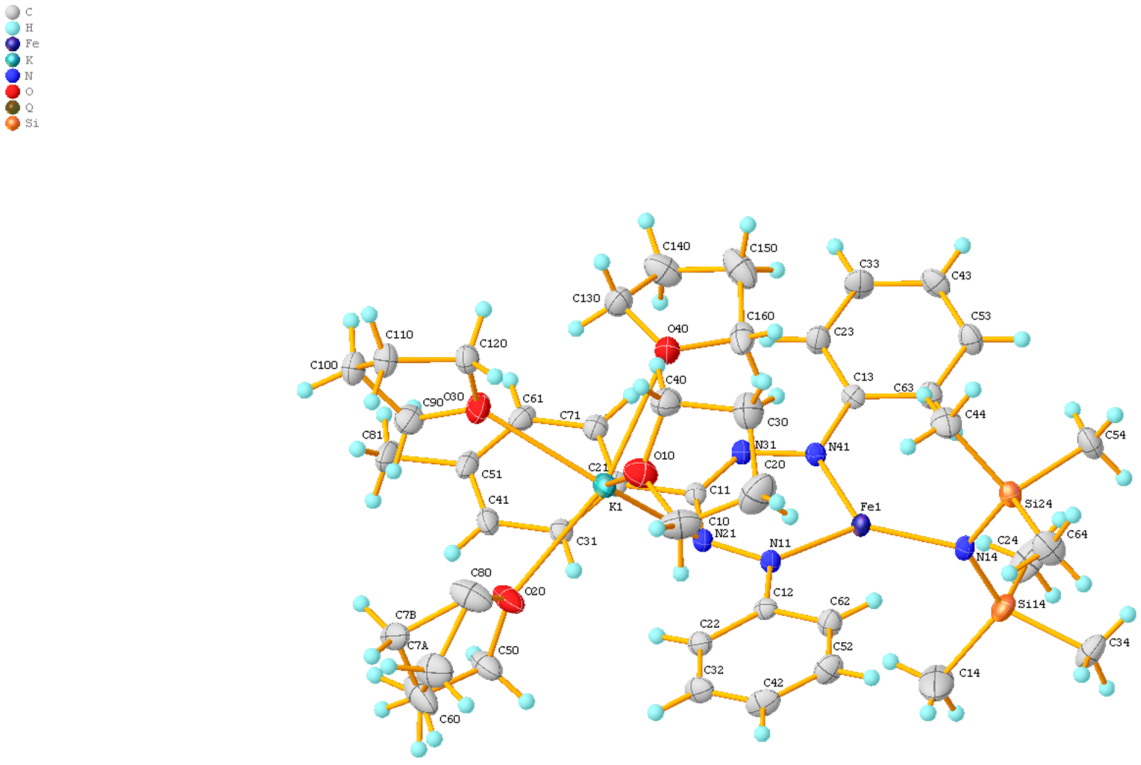

Figure S21. The complete numbering scheme of **4-K** with 50% thermal ellipsoid probability levels. The hydrogen atoms are shown as circles for clarity.

Table S3. Crystal data and structure refinement for **4-K**.

Identification code	007c-17023	
Empirical formula	C42 H65 Fe K N5 O4 Si2	
Formula weight	855.12	
Temperature	93(2) K	
Wavelength	0.71073 Å	
Crystal system	Triclinic	
Space group	P-1	
Unit cell dimensions	a = 11.2204(3) Å	α= 85.3384(19)°.
	b = 13.7762(3) Å	β= 81.919(2)°.
	c = 16.4107(4) Å	γ = 67.220(2)°.
Volume	2314.57(10) $Å^3$	
Z	2	
Density (calculated)	1.227 g/cm^3	
Absorption coefficient	0.511 mm^{-1}	
F(000)	914	
Crystal size	0.200 x 0.200 x 0.200 mm^3	
Crystal color and habit	Black Block	
Diffractometer	Dectris Pilatus 3R	
Theta range for data collection	2.938 to 27.484°.	
Index ranges	-14<=h<=14, -17<=k<=17, -21<=l<=21	
Reflections collected	61840	
Independent reflections	10606 [R(int) = 0.0361]	
Observed reflections (I > 2sigma(I))	9214	
Completeness to theta = 25.242°	99.9 %	
Absorption correction	Semi-empirical from equivalents	
Max. and min. transmission	1.00000 and 0.90532	
Solution method	SHELXT-2014/5 (Sheldrick, 2014)	
Refinement method	SHELXL-2014/7 (Sheldrick, 2014)	
Data / restraints / parameters	10606 / 0 / 512	
Goodness-of-fit on F^2	1.038	
Final R indices [I>2sigma(I)]	R1 = 0.0306, wR2 = 0.0781	
R indices (all data)	R1 = 0.0375, wR2 = 0.0807	
Largest diff. peak and hole	0.594 and -0.317 $e.Å^{-3}$	

3-K

Low-temperature diffraction data (ω-scans) were collected on a Rigaku MicroMax-007HF diffractometer coupled to a Saturn994+ CCD detector with Cu Kα (λ = 1.54178 Å) for the structure of **3-K**. The diffraction images were processed and scaled using Rigaku Oxford Diffraction software (CrysAlisPro; Rigaku OD: The Woodlands, TX, 2015). The structure was solved with SHELXT and was refined against F^2 on all data by full-matrix least squares with SHELXL (Sheldrick, G. M. Acta Cryst. 2008, A64, 112–122). All non-hydrogen atoms were refined anisotropically. Hydrogen atoms were included in the model at geometrically calculated positions and refined using a riding model. The isotropic displacement parameters of all hydrogen atoms were fixed to 1.2 times the U value of the atoms to which they are linked (1.5 times for methyl groups). Two THF molecules have disordered carbon positions. C20 and C23 have split positions. There major and minor sites are distinguished with the suffixes "A" and "B", respectively. The site occupancies for these sites converged to values of 0.60(3) and 0.40(3). The hydrogen atoms associated with the disordered positions were geometrically generated as riding atoms. All chemically equivalent C-C bonds were restrained to be similar. There appears to be at least 4 sites in the asymmetric unit that are occupied by solvent. However, 2 sites are disordered across a crystallographic inversion and all of these solvent sites show signs of disorder. The 2, fully occupied sites on general positions appear to be THF molecules. There atomic parameters are copied below:

A1 -0.27049 -1.34018 -0.64133
A2 -0.37110 -1.31236 -0.66849
A3 -0.39627 -1.38335 -0.68654
A4 -0.31655 -1.45760 -0.66683
A5 -0.23653 -1.42140 -0.65961

A6 -0.89274 -1.37556 -0.40273
A7 -0.85120 -1.35270 -0.45822
A8 -0.76242 -1.30505 -0.45017
A9 -0.77989 -1.28121 -0.39970
A10 -0.83825 -1.34831 -0.36094

The other two sites near crystallographic inversions could be either pentane or THF. Ultimately, the program SQUEEZE was used to compensate for the contribution of all disordered solvents contained in voids within the crystal lattice. This procedure was applied to the data file and the submitted model is based on the solvent removed data. Based on the total electron density found in the voids (272.5 e/Å^3), it is likely that ~6 pentane molecules, ~6 THF molecules, or some combination of these solvents are present in the unit cell. See "_platon_squeeze_details" in this .cif for more information. The full numbering scheme of compound **3-K** can be found in the full details of the X-ray structure determination (CIF), which is included as Supporting Information. CCDC number 1815891 (**3-K**) contains the supplementary crystallographic data for this paper. These data can be obtained free of charge from The Cambridge Crystallographic Data Center via www.ccdc.cam.ac.uk/data_request/cif.

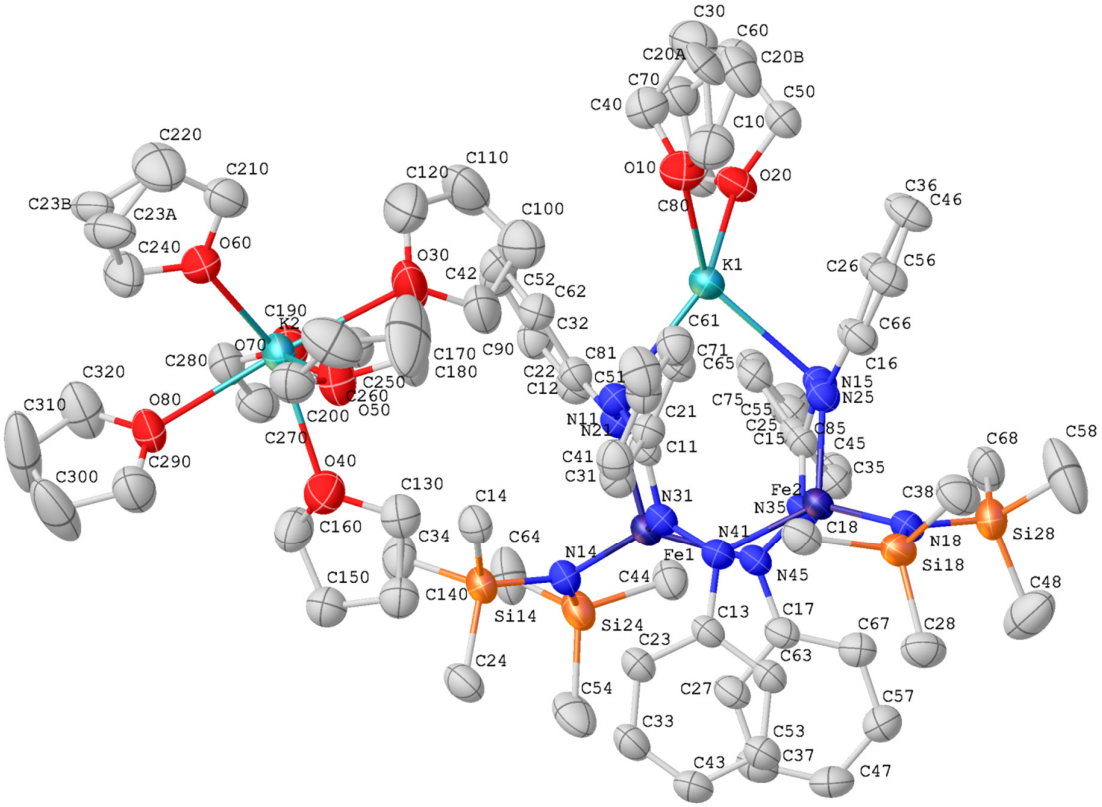

Figure S22. The complete numbering scheme of **3-K** with 50% thermal ellipsoid probability levels. The hydrogen are omitted for clarity.

Table S4. Crystal data and structure refinement for **3-K**.

Identification code	007b-17100	
Empirical formula	C84 H131 Fe2 K2 N10 O8 Si4	
Formula weight	1711.24	
Temperature	93(2) K	
Wavelength	1.54178 Å	
Crystal system	Triclinic	
Space group	P-1	
Unit cell dimensions	a = 14.2192(4) Å	α= 71.795(2)°.
	b = 15.8275(6) Å	β= 87.428(2)°.
	c = 24.5777(4) Å	γ = 83.095(3)°.
Volume	5216.2(3) $Å^3$	
Z	2	
Density (calculated)	1.090 g/cm^3	
Absorption coefficient	3.776 mm^{-1}	
F(000)	1830	
Crystal size	0.120 x 0.040 x 0.010 mm^3	
Crystal color and habit	Red Plate	
Diffractometer	Rigaku Saturn 944+ CCD	
Theta range for data collection	1.892 to 66.590°.	
Index ranges	-16<=h<=16, -18<=k<=18, -29<=l<=29	
Reflections collected	178338	
Independent reflections	18160 [R(int) = 0.2055]	
Observed reflections (I > 2sigma(I))	14176	
Completeness to theta = 66.590°	98.5 %	
Absorption correction	None	
Solution method	SHELXT-2014/5 (Sheldrick, 2014)	
Refinement method	SHELXL-2014/7 (Sheldrick, 2014)	
Data / restraints / parameters	18160 / 45 / 1026	
Goodness-of-fit on F^2	1.157	
Final R indices [I>2sigma(I)]	R1 = 0.0903, wR2 = 0.2571	
R indices (all data)	R1 = 0.1090, wR2 = 0.2944	
Extinction coefficient	0.0025(2)	
Largest diff. peak and hole	0.930 and -1.308 $e.Å^{-3}$	

3-Rb

Low-temperature diffraction data (ω-scans) were collected on a Rigaku MicroMax-007HF diffractometer coupled to a Dectris Pilatus3R detector with Mo Kα (λ = 0.71073 Å) for the structure of **3-Rb**. The diffraction images were processed and scaled using Rigaku Oxford Diffraction software (CrysAlisPro; Rigaku OD: The Woodlands, TX, 2015). The structure was solved with SHELXT and was refined against F^2 on all data by full-matrix least squares with SHELXL (Sheldrick, G. M. Acta Cryst. 2008, A64, 112–122). All non-hydrogen atoms were refined anisotropically. Hydrogen atoms were included in the model at geometrically calculated positions and refined using a riding model. The isotropic displacement parameters of all hydrogen atoms were fixed to 1.2 times the U value of the atoms to which they are linked (1.5 times for methyl groups). Three THF molecules and one TMS functional group show signs of disorder based on the difference map. For THF, The difference map suggest only two sites for disordered atom positions. The site occupancies of these atoms were freely refined to converged values. In all cases, the disordered pairs were nearly equal in their site occupancies. The disordered TMS group was also modeled over two positions, but the freely refined site occupancies converged near a 0.75:0.25 split. All disordered C-C, C-O and Si-C bond distances that were chemically identical were restrained to be similar. The program SQUEEZE was used to compensate for the contribution of disordered solvents contained in voids within the crystal lattice from the diffraction intensities. This procedure was applied to the data file and the submitted model is based on the solvent removed data. Based on the total electron density found in the voids (258 e/Å^3), it is likely that ~6.5 THF molecules are present in the unit cell. See "_platon_squeeze_details" in this .cif for more information. The full numbering scheme of compound **3-Rb** can be found in the full details of the X-ray structure determination (CIF), which is included as Supporting Information. CCDC number 1815889 (**3-Rb**) contains the supplementary crystallographic data for this paper. These data can be obtained free of charge from The Cambridge Crystallographic Data Center via www.ccdc.cam.ac.uk/data_request/cif.

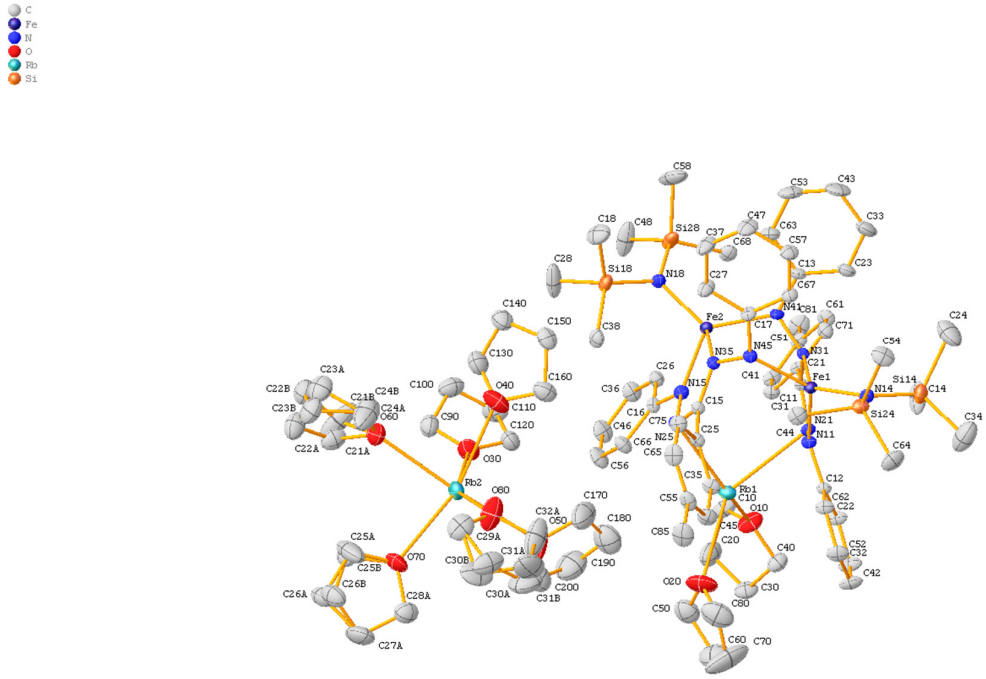

Figure S23. The complete numbering scheme of **3-Rb** with 50% thermal ellipsoid probability levels. The hydrogen atoms are omitted for clarity.

Table S5. Crystal data and structure refinement for **3-Rb**.

Identification code	007c-17024	
Empirical formula	C84 H134 Fe2 N10 O8 Rb2 Si4	
Formula weight	1807.00	
Temperature	93(2) K	
Wavelength	0.71073 Å	
Crystal system	Triclinic	
Space group	P-1	
Unit cell dimensions	a = 14.2536(3) Å	α= 72.387(2)°.
	b = 15.8670(3) Å	β= 87.489(2)°.
	c = 24.6478(6) Å	γ = 83.894(2)°.
Volume	5282.5(2) $Å^3$	
Z	2	
Density (calculated)	1.136 g/cm^3	
Absorption coefficient	1.284 mm^{-1}	
F(000)	1908	
Crystal size	0.200 x 0.100 x 0.020 mm^3	
Crystal color and habit	Black Plate	
Diffractometer	Dectris Pilatus 3R	
Theta range for data collection	2.875 to 27.103°.	
Index ranges	-18<=h<=18, -20<=k<=20, -31<=l<=27	
Reflections collected	139573	
Independent reflections	23289 [R(int) = 0.0451]	
Observed reflections (I > 2sigma(I))	19062	
Completeness to theta = 25.242°	99.8 %	
Absorption correction	Semi-empirical from equivalents	
Max. and min. transmission	1.00000 and 0.83165	
Solution method	SHELXT-2014/5 (Sheldrick, 2014)	
Refinement method	SHELXL-2014/7 (Sheldrick, 2014)	
Data / restraints / parameters	23289 / 100 / 1111	
Goodness-of-fit on F^2	1.037	
Final R indices [I>2sigma(I)]	R1 = 0.0378, wR2 = 0.0760	
R indices (all data)	R1 = 0.0513, wR2 = 0.0794	
Largest diff. peak and hole	0.507 and -0.415 $e.Å^{-3}$	

3-Cs

Low-temperature diffraction data (ω-scans) were collected on a Rigaku MicroMax-007HF diffractometer coupled to a Dectris Pilatus3R detector with Mo Kα (λ = 0.71073 Å) for the structure of **3-Cs**. The diffraction images were processed and scaled using Rigaku Oxford Diffraction software (CrysAlisPro; Rigaku OD: The Woodlands, TX, 2015). The structure was solved with SHELXT and was refined against F^2 on all data by full-matrix least squares with SHELXL (Sheldrick, G. M. Acta Cryst. 2008, A64, 112–122). All non-hydrogen atoms were refined anisotropically. Hydrogen atoms were included in the model at geometrically calculated positions and refined using a riding model. The isotropic displacement parameters of all hydrogen atoms were fixed to 1.2 times the U value of the atoms to which they are linked (1.5 times for methyl groups). The initial solution appeared to be ordered with some possible sites of disorder in the THF molecules coordinated to the Cs. However, the difference had seemingly random peaks in chemically unreasonable positions. The distances between the largest difference map peaks (Q1: 9.03 Q2: 8.55) was 5.9419(2) Angstroms. This is similar to the distance found between Cs1-Cs2: 5.8259(2) Angstroms. These two difference map peaks were modeled as disordered Cs atoms Cs1b and Cs2b. Their site occupancies were freely refined and suggested an occupancy of 0.03. The site occupancies were fixed and the thermal parameters were constrained to be the same as Cs1 and Cs2. A second set of large difference map peaks (Q1: 4.97 Q4: 4.44) appeared after the Cs atoms were modeled as disordered. The distance between Q1 and Q2 is 3.94974(14). This is similar to the Fe1-Fe2 distance of 3.97824(14).

It is possible that there is whole molecule disorder of the complex. Using orthogonal coordinates of the major orientation as a templet did not provide a stable model of whole molecule disorder. The Cs atoms were left modeled as disordered, but the remaining atoms were refined at full occupancy. The sites Q1, Q2 and other large difference map peaks were left without a model. The full numbering scheme of compound **3-Cs** can be found in the full details of the X-ray structure determination (CIF), which is included as Supporting Information. CCDC number 1815892 (**3-Cs**) contains the supplementary crystallographic data for this paper. These data can be obtained free of charge from The Cambridge Crystallographic Data Center via www.ccdc.cam.ac.uk/data_request/cif.

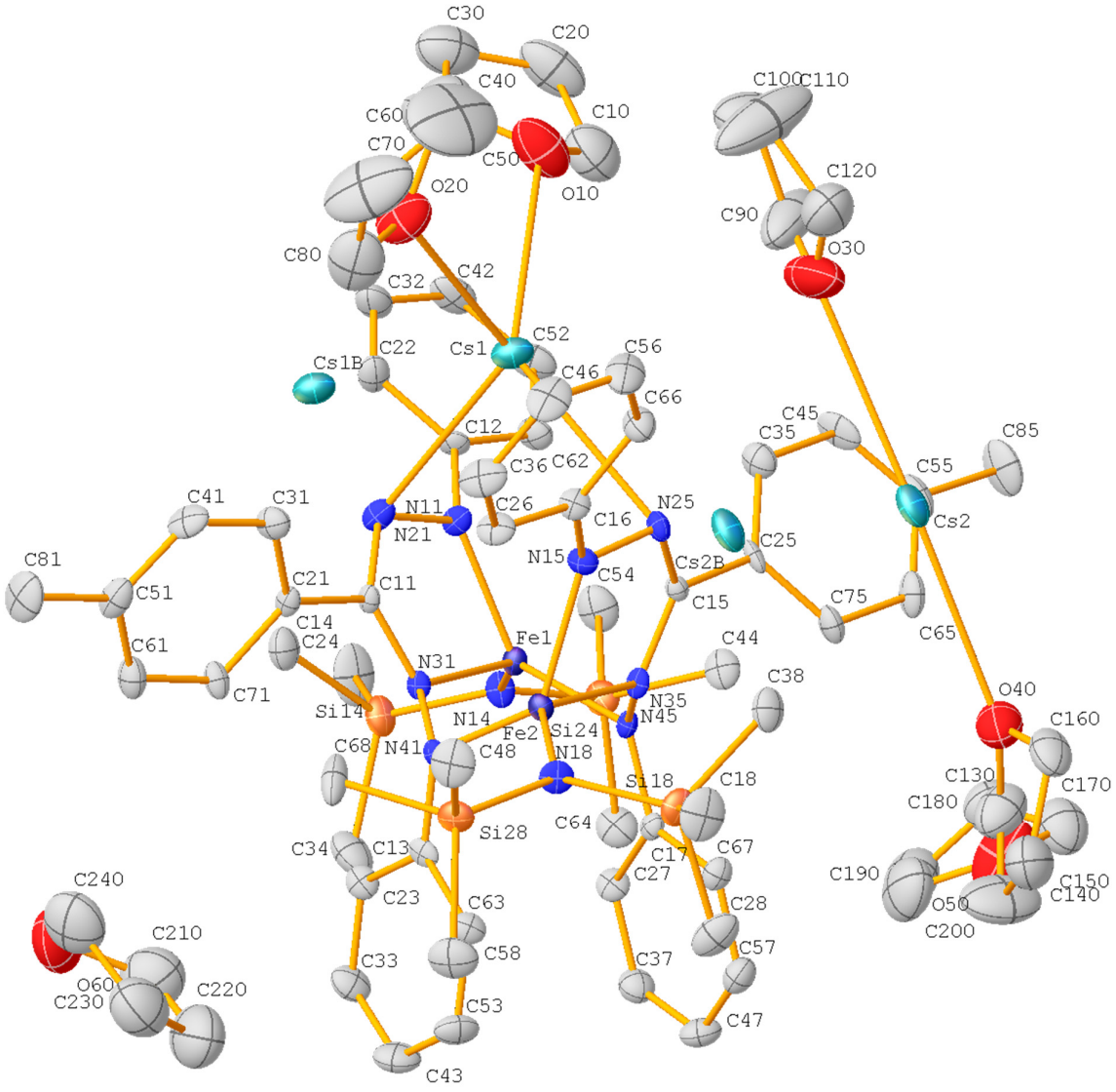

Figure S24. The complete numbering scheme of **3-Cs** with 50% thermal ellipsoid probability levels. The hydrogen atoms are omitted for clarity.

Table S6. Crystal data and structure refinement for **3-Cs**

Identification code	007c-17029	
Empirical formula	C76 H118 Cs2 Fe2 N10 O6 Si4	
Formula weight	1757.68	
Temperature	93(2) K	
Wavelength	0.71073 Å	
Crystal system	Monoclinic	
Space group	$P2_1/n$	
Unit cell dimensions	a = 16.5108(6) Å	α= 90°.
	b = 28.2982(9) Å	β= 100.033(3)°.
	c = 18.1722(6) Å	γ = 90°.
Volume	8360.7(5) $Å^3$	
Z	4	
Density (calculated)	1.396 g/cm^3	
Absorption coefficient	1.317 mm^{-1}	
F(000)	3640	
Crystal size	0.100 x 0.050 x 0.010 mm^3	
Crystal color and habit	black plate	
Diffractometer	Dectris Pilatus 3R	
Theta range for data collection	2.798 to 27.484°.	
Index ranges	-21<=h<=21, -36<=k<=36, -23<=l<=23	
Reflections collected	163518	
Independent reflections	19157 [R(int) = 0.1434]	
Observed reflections (I > 2sigma(I))	13979	
Completeness to theta = 25.242°	99.9 %	
Absorption correction	Semi-empirical from equivalents	
Max. and min. transmission	1.00000 and 0.26741	
Solution method	SHELXT-2014/5 (Sheldrick, 2014)	
Refinement method	SHELXL-2014/7 (Sheldrick, 2014)	
Data / restraints / parameters	19157 / 0 / 921	
Goodness-of-fit on F^2	1.082	
Final R indices [I>2sigma(I)]	R1 = 0.0826, wR2 = 0.2135	
R indices (all data)	R1 = 0.1125, wR2 = 0.2325	
Largest diff. peak and hole	4.967 and -1.564 $e.Å^{-3}$	

Calculations. All calculations were performed with the electronic structure program ORCA.[6] Single-point DFT calculations used the B3LYP[7] hybrid functional on the crystallographic coordinates of **3-Na** with counterions and solvent molecules removed. The scalar relativistically recontracted def2-TZVP(-f) were used all atoms and enhanced integration accuracy was used for iron (SPECIALGRIDINTACC 7).[8] Calculations with hybrid functionals used the RIJCOSX algorithm to speed the calculation of Hartree–Fock exchange.[9] Calculations included the zeroth-order regular approximation (ZORA) for relativistic effects[10] as implemented by van Wüllen.[11] Auxiliary basis sets for all complexes used to expand the electron density in the calculations were chosen to match the orbital basis. The self-consistent field (SCF) calculations were tightly converged (1×10^{-8} E_h in energy, 1×10^{-7} E_h in the density change, and 1×10^{-7} in the maximum element of the DIIS[12] error vector). The geometry search for all complexes was carried out in redundant internal coordinates without imposing geometry constraints. We used the broken symmetry (BS) approach to describe our computational results for all compounds.[13] We adopted the following notation: the given system was divided into two fragments. The notation BS(m,n) refers then to a broken symmetry state with m unpaired α-spin electrons essentially on fragment 1 and n unpaired β-spin electrons localized on fragment 2. In each case, fragments 1 and 2 correspond to the two metal ions. In this notation the standard high spin, open-shell solution is written as BS(m+n,0). The BS(m,n) notation refers to the initial guess to the wavefunction. The variational process does, however, have the freedom to converge to a solution of the form BS(m−n,0) in which effectively the n β-spin electrons pair up with $n < m$ α-spin electrons on the partner fragment. Such a solution is then a standard $M_S \approx (m-n)/2$ spin-unrestricted Kohn-Sham solution. The nature of the solution is investigated from the corresponding orbital transformation[14] which, from the corresponding orbital overlaps, displays whether the system should be described as a spin-coupled or a closed-shell solution. Molecular orbitals and spin density maps were visualized via the program Molekel.[15]

References

[1] Broere, D. L. J.; Mercado, B. Q.; Lukens, J. T.; Vilbert, A. C.; Banerjee, G.; Lant, H. M. C.; Lee, S. H.; Bill, E.; Sproules, S.; Lancaster, K. M.; Holland, P. L. H. Redox-Active Formazanates in Low-Coordinate Iron Chemistry. *Submitted.*

[2] Dresselhaus, M. S.; Dresselhaus, G. Intercalation compounds of graphite. *Adv. Phys.* **1981**, *30*, 139-326.

[3] Amman, C; Meier, P.; Merbach, A. E. A simple multinuclear NMR thermometer. *J. Magn. Reson.* **1982**, *46*, 319-321.

[4] Travieso-Puente, R.; Broekman, J. O. P.; Chang, M.-C.; Demeshko, S.; Meyer, F.; Otten, E. Spin-Crossover in a Pseudo-tetrahedral Bis (formazanate) Iron Complex. *J. Am. Chem. Soc.* **2016**, *138*, 5503-5506.

[5] George, G. N. *EXAFSPAK*; Stanford Synchrotron Radiation Lightsource, Stanford Linear Accelerator Center; Stanford University: Stanford, CA, 2001.

[6] Neese, F. The ORCA program system. *WIREs Comput. Molec. Sci.*, **2012**, *2*, 73–78.

[7] (a) Becke, A. D. Density-functional thermochemistry. III. The role of exact exchange. *J. Chem. Phys.* **1993**, *98*, 5648–5652. (b) Lee, C. T.; Yang, W. T.; Parr, R. G. Development of the Colle-Salvetti correlation-energy formula into a functional of the electron density. *Phys. Rev. B* **1988**, *37*, 785–789.

[8] (a) Weigend, F.; Ahlrichs, R. Balanced basis sets of split valence, triple zeta valence and quadruple zeta valence quality for H to Rn: Design and assessment of accuracy. *Phys. Chem. Chem. Phys.* **2005**, *7*, 3297–3305. (b) Pantazis, D. A.; Chen, X.-Y.; Landis, C. R.; Neese, F. All-electron scalar relativistic basis sets for third-row transition metal atoms. *J. Chem. Theory Comput.* **2008**, *4*, 908–919.

[9] (a) Neese, F.; Wennmohs, F.; Hansen, A. Efficient and accurate local approximations to coupled-electron pair approaches: An attempt to revive the pair natural orbital method. *J. Chem. Phys.* **2009**, *130*, 114108. (b) Izsák, R.; Neese, F. An overlap fitted chain of spheres exchange method. *J. Chem. Phys.* **2011**, *135*, 144105.

[10] (a) van Lenthe, E.; Snijders, J. G.; Baerends, E. J. The zero-order regular approximation for relativistic effects: The effect of spin–orbit coupling in closed shell molecules. *J. Chem. Phys.* **1996**, *105*, 6505–6516. (b) van Lenthe, J. H.; Faas, S.; Snijders, J. G. Gradients in the ab initio scalar zeroth-order regular approximation (ZORA) approach. *Chem. Phys. Lett.* **2000**, *328*, 107–112. (c) van Lenthe, E.; van der Avoird, A.; Wormer, P. E. S. Density functional calculations of molecular hyperfine interactions in the zero order regular approximation for relativistic effects. *J. Chem. Phys.* **1998**, *108*, 4783–4796.

[11] van Wüllen, C. Molecular density functional calculations in the regular relativistic approximation: Method, application to coinage metal diatomics, hydrides, fluorides and chlorides, and comparison with first-order relativistic calculations. *J. Chem. Phys.* **1998**, *109*, 392–399.

[12] (a) Pulay, P. Convergence acceleration of iterative sequences. The case of SCF iteration. *Chem. Phys. Lett.* **1980**, *73*, 393–398. (b) Pulay, P. Improved SCF convergence acceleration. *J. Comput. Chem.* **1982**, *3*, 556–560.

[13] (a) Noodleman, L. Valence bond description of antiferromagnetic coupling in transition metal dimers. *J. Chem. Phys.* **1981**, *74*, 5737–5743. (b) Noodleman, L.; Case, D. A.; Aizman, A. Broken symmetry analysis of spin coupling in iron-sulfur clusters. *J. Am. Chem. Soc.* **1988**, *110*, 1001–1005. (c) Noodleman, L.; Davidson, E. R. Ligand spin polarization and antiferromagnetic coupling in transition metal dimers. *Chem. Phys.* **1986**, *109*, 131–143. (d) Noodleman, L.; Norman, J. G.; Osborne, J. H.; Aizman, A.; Case, D. A. Models for ferredoxins: electronic structures of iron-sulfur clusters with

one, two, and four iron atoms. *J. Am. Chem. Soc.* **1985**, *107*, 3418–3426. (e) Noodleman, L.; Peng, C. Y.; Case, D. A.; Monesca, J. M. Orbital interactions, electron delocalization and spin coupling in iron-sulfur clusters. *Coord. Chem. Rev.* **1995**, *144*, 199–244.

[14] Neese, F. Definition of corresponding orbitals and the diradical character in broken symmetry DFT calculations on spin coupled systems. *J. Phys. Chem. Solids* **2004**, *65*, 781–785.

[15] *Molekel*, Advanced Interactive 3D-Graphics for Molecular Sciences, Swiss National Supercomputing Centre. https://ugovaretto.github.io/molekel/